

This discussion paper is/has been under review for the journal Atmospheric Chemistry and Physics (ACP). Please refer to the corresponding final paper in ACP if available.

Characterizing the impact of urban emissions on regional aerosol particles; airborne measurements during the MEGAPOLI experiment

E. J. Freney¹, K. Sellegri¹, F. Canonaco², A. Colomb¹, A. Borbon³, V. Michoud³, J.-F. Doussin³, S. Crumeyrolle⁴, N. Amarouch⁵, J.-M. Pichon¹, A. S. H. Prévôt², M. Beekmann³, and A. Schwarzenböck¹

¹Laboratoire de Météorologie Physique, CNRS-Université Blaise Pascal, UMR6016, 63117, Clermont Ferrand, France

²Paul Scherrer Institute, Laboratory of Atmospheric Chemistry, 5232 Villigen PSI, Switzerland

³Laboratoire Interuniversitaire des Systemes Atmosphériques, LISA/IPSL, UMR CNRS 7583, Université Paris Est Creteil (UPEC) and Université Paris Diderot (UPD), France

⁴NASA Langley Research Center, Hampton, VA 23681, USA

⁵CNRS, Div Tech, Inst Natl Sci Univers, UPS 855, 92195 Meudon, France

Impact of urban emissions on regional aerosol particles

E. J. Freney et al.

Title Page

Abstract

Introduction

Conclusions

References

Tables

Figures

⏪

⏩

◀

▶

Back

Close

Full Screen / Esc

Printer-friendly Version

Interactive Discussion

Received: 11 July 2013 – Accepted: 6 September 2013 – Published: 24 September 2013

Correspondence to: E. J. Freney (e.freney@opgc.univ-bpclermont.fr)

Published by Copernicus Publications on behalf of the European Geosciences Union.

ACPD

13, 24885–24924, 2013

Impact of urban emissions on regional aerosol particles

E. J. Freney et al.

Title Page

Abstract

Introduction

Conclusions

References

Tables

Figures



Back

Close

Full Screen / Esc

Printer-friendly Version

Interactive Discussion



Abstract

The MEGAPOLI experiment took place in July 2009. The aim of this campaign was to study the aging and reactions of aerosol and gas-phase emissions in the city of Paris. Three ground-based measurement sites and several mobile platforms including instrument equipped vehicles and the ATR-42 aircraft were involved. We present here the variations in particle- and gas-phase species over the city of Paris using a combination of high-time resolution measurements aboard the ATR-42 aircraft. Particle chemical composition was measured using a compact time-of-flight aerosol mass spectrometer (C-ToF-AMS) giving detailed information of the non-refractory submicron aerosol species. The mass concentration of BC, measured by a particle absorption soot photometer (PSAP), was used as a marker to identify the urban pollution plume boundaries. Aerosol mass concentrations and composition were affected by air-mass history, with air masses that spent longest time over land having highest fractions of organic aerosol and higher total mass concentrations. The Paris plume is mainly composed of organic aerosol (OA), black carbon and nitrate aerosol, as well as high concentrations of anthropogenic gas-phase species such as toluene, benzene, and NO_x . Using BC and CO as tracers for air-mass dilution, we observe the ratio of $\Delta\text{OA} / \Delta\text{BC}$ and $\Delta\text{OA} / \Delta\text{CO}$ increase with increasing photochemical age ($-\log(\text{NO}_x / \text{NO}_y)$). Plotting the equivalent ratios for the Positive Matrix Factorization (PMF) resolved species (LV-OOA, SV-OOA, and HOA) illustrate that the increase in OA is a result of secondary organic aerosol (SOA). Within Paris the changes in the $\Delta\text{OA} / \Delta\text{CO}$ are similar to those observed during other studies in Mexico city, Mexico and in New England, USA. Using the measured VOCs species together with recent organic aerosol formation yields we predicted $\sim 50\%$ of the measured organics. These airborne measurements during the MEGAPOLI experiment show that urban emissions contribute to the formation of OA, and have an impact on aerosol composition on a regional scale. They provide a quantitative measure of this impact in terms of urban plume composition and evolution relative to background aerosol composition.

24887

ACPD

13, 24885–24924, 2013

Impact of urban emissions on regional aerosol particles

E. J. Freney et al.

Title Page

Abstract

Introduction

Conclusions

References

Tables

Figures

⏪

⏩

◀

▶

Back

Close

Full Screen / Esc

Printer-friendly Version

Interactive Discussion



Impact of urban emissions on regional aerosol particles

E. J. Freney et al.

Title Page

Abstract

Introduction

Conclusions

References

Tables

Figures

⏪

⏩

◀

▶

Back

Close

Full Screen / Esc

Printer-friendly Version

Interactive Discussion

its favorable geographical situation (far from other big European cities and influenced very often by clean oceanic air masses), it is a good candidate for investigating the build-up of the urban contribution to the regional air pollution burden. In recent years, there have been increases in air quality studies within the Paris region using both measurement and modeling tools (Sciare et al., 2010; Hodzic et al., 2005; Zhang et al., 2013). Important conclusions of these studies include the need for size-resolved composition measurements of $PM_{2.5}$ aerosol, as well as the need of vertical measurements of aerosol species. Particulate mass of fine aerosols ($PM_{2.5}$) is continuously monitored at several sites within Greater Paris for almost 8 yr by the local air quality network (AIR-PARIF). However, dedicated measurements of aerosol composition in the urban plume have never been performed.

The FP7/MEGAPOLI project (Megacities: emissions, urban, regional and global atmospheric pollution and climate effects, and integrated tool for assessment and mitigation, 2008 to 2011) is aimed at improving the understanding of the impact of megacities on air quality on a local, regional, and global scale (Baklanov et al., 2010). It additionally aims to improve our understanding of the relationships existing between air quality and climatic change on both a local and regional scale. In this framework, two large field experiments were realized in the Greater Paris region, in summer 2009 and winter 2010. Freutel et al. (2013) and Crippa et al. (2013a) described the chemical composition of aerosol particles measured at the ground based sites during the summer and winter campaigns, respectively. Here we discuss airborne measurements of the main chemical constituents of PM_1 within the city plume. Local and regional contributions to the major chemical constituents of PM_1 are discussed together with back trajectory air mass analysis and compared with variations in the concentration of volatile organic compounds (VOC) and other gas-phase species.

2 Materials and methods

2.1 ATR-42 aircraft

All measurements were performed aboard the ATR-42, a French national research aircraft run by SAFIRE (French aircraft service for environmental research). The ATR-42 is equipped to perform measurements of meteorology, particles, gas, and clouds. The different meteorological variables measured include temperature, dew point temperature, pressure, turbulence, relative humidity, wind speed, and direction. Gas- and particle-phase species were sampled through a forward-facing inlet installed in place of a side window of the aircraft. The inlet is composed of an outer sleeve for channeling air and a tube radius of curvature high enough to limit losses during transport of particles (Crumeyrolle et al., 2008). Before aerosol particles were sampled into the C-ToF-AMS they passed through a pressure controlled inlet (PCI). The PCI ensured a constant pressure at the inlet of the C-ToF-AMS (1.26 torr) and avoids pressure changes to the aerodynamic inlet of the C-ToF-AMS during airborne sampling (Bahreini et al., 2008).

For BC measurements, a particle soot absorption photometer (Radiance research)[®] (PSAP), measured the particle absorption coefficient at 565 nm with a time resolution of 60 s. Filters were changed prior to each flight to ensure that transmission efficiency was greater than 80 %. A scanning mobility particle sizer (SMPS) measured the mobility diameter of aerosol particles from 30 to 500 nm with a resolution of 84 s.

2.2 Aerosol chemistry measurements

The chemical composition and mass concentration of the non-refractory submicron particulate matter (NR-PM₁) was measured with an Aerodyne C-ToF-AMS with a time resolution of 36 s (Drewnick et al., 2005; Canagaratna et al., 2007). In order to extract chemically resolved mass concentrations of individual species, the C-ToF-AMS raw data are evaluated using the standard fragmentation table (Allan et al., 2004). Adjustments to the fragmentation table were made based on particle-free measurement peri-

Impact of urban emissions on regional aerosol particles

E. J. Freney et al.

Title Page

Abstract

Introduction

Conclusions

References

Tables

Figures

⏪

⏩

◀

▶

Back

Close

Full Screen / Esc

Printer-friendly Version

Interactive Discussion

Impact of urban emissions on regional aerosol particles

E. J. Freney et al.

Title Page

Abstract

Introduction

Conclusions

References

Tables

Figures

⏪

⏩

◀

▶

Back

Close

Full Screen / Esc

Printer-friendly Version

Interactive Discussion



ods that were performed during each flight. The resolved mass concentrations include nitrate (NH_4), sulfate (SO_4), Ammonium (NO_3), Organics (Org), and Chloride (Chl) species. Ionization efficiency (IE) calibrations, using ammonium nitrate, were made after each research flight giving IE values of $2.0 \pm 0.5 \times 10^{-7}$ for nitrate.

The calculation of quantitative mass concentrations from the C-ToF-AMS mass spectra requires that a collection efficiency (CE) be applied to the data. The CE is defined as the fraction of the particle mass that is measured by the AMS, relative to what would have been measured if all particles were spherical and particle bounce was negligible. Recently, it has been demonstrated that particles containing high ammonium nitrate concentrations are more efficiently sampled by the C-ToF-AMS than other inorganic and organic species (Middlebrook et al., 2011). It is therefore recommended that a composition dependent CE be applied to the data (Eq. 1).

$$\text{CE}_{\text{DRY}} = \max(0.5, 0.264 + 0.943 X \text{ANMF}) \quad (1)$$

in which a constant CE of 0.5 is used for ammonium nitrate mass fraction ($\text{ANMF} \leq 0.25$ and a linear CE increase up to 1 for $\text{ANMF} \geq 0.25$ (Freney et al., 2011) ($\text{CE} = 1$, for $\text{ANMF} = 1$). In order to validate our chosen CE, we compared the total volume of aerosol particles sampled by the C-ToF-AMS and BC with that sampled by a scanning mobility particle sizer (SMPS). The C-ToF-AMS volume was calculated by dividing the mass concentrations of organic and inorganic species by their respective densities (1.72 g m^{-3} for SO_4 , NH_4 , NO_3 , and 1.2 g m^{-3} for organics). Comparing the total mass concentration measured by the C-ToF-AMS and BC for all research flights with the corresponding SMPS measurements we obtain a correlation with an average r^2 and slope of 0.71 ± 0.14 and 0.98 ± 0.073 respectively (Fig. S1).

2.2.1 PMF analysis

Positive matrix factorisation (PMF) (Paatero and Tapper, 1994; Paatero, 1997) was performed with PMF2 software package (P. Paatero, University of Helsinki, Finland)

0.58 $\mu\text{g m}^{-3}$, with lowest values measured during easterly flights and highest during northerly flights.

Similar procedures were performed for OA and CO concentrations. Care needs to be taken in defining the background values in order to calculate accurate values of $\Delta\text{OA}/\Delta\text{CO}$ or $\Delta\text{OA}/\Delta\text{BC}$ (Sect. 3.3.2). Subtracting too large background values can skew these ratios to either very large or very small values.

2.3 Gas-phase measurements.

CO and O₃ were sampled through a rear-facing 1/4 inch Teflon tube and were measured using infra-red and ultra-violet analysers (Thermal-environmental instruments), respectively (Nedelec et al., 2003). NO and NO₂ were sampled through a separate rear-facing pressure controlled inlet at a 30 s time resolution and measured using the MONA instrument based on ozone chemiluminescence and developed by the Laboratoire Interuniversitaire des Systems Atmospheres (LISA), Paris. NO_y measurements are performed using a separate heated (60 °C) sampling line to avoid any loss of nitric acid. The air then passes through a gold converter (8 mm inox tube cover of gold) heated to 200 °C with H₂ as a reagent to convert nitrogen species into NO. Additional details of the MONA instrument are supplied in the supplementary material.

An airborne proton transfer reaction mass spectrometer (PTR-MS) instrument was deployed on board the ATR-42 for the first time, providing measurements on the volatile organic carbon (VOC) in the atmosphere. A high sensitivity PTR-MS from Ionicon Analytik (Innsbruck, Austria) was re-designed to fit in an ATR-42 rack to meet aircraft safety rules. Typical background counts for aromatics were between 0.8 and 10 counts s⁻¹. Detection limits, defined as the 1 σ variability in the background mixing ratios, were between 0.070 ppb and 0.150 ppb for a 2 s-dwell time. A scheme of the PTR-MS configuration and operating conditions including calibration protocols on-board are provided in Borbon et al. (2012).

Impact of urban emissions on regional aerosol particles

E. J. Freney et al.

Title Page

Abstract

Introduction

Conclusions

References

Tables

Figures

⏪

⏩

◀

▶

Back

Close

Full Screen / Esc

Printer-friendly Version

Interactive Discussion



2.4 Back trajectory analysis

In order to determine the transport pathways of the aerosol particles prior to arriving along the flight track (700 m), the Hybrid Single Particle Lagrangian Trajectory (HYS-PLIT) model was used (Draxler and Hess, 1998). Air mass backward trajectories were calculated for the arrival pressure level of 950 hPa and were calculated every six hours, the first starting at 00:00 UTC time. Air masses were followed 72 h backwards in one hour time steps. Figure 1 shows examples of trajectories calculated for four flights. The map of Europe is separated into grid squares with a 1° resolution. Each grid square is coloured by the amount of time that the air-mass spent in that area.

3 Results and discussion

A total of 8 research flights (RFs) with reliable C-ToF-AMS measurements are available aboard the ATR-42 from 13 to 29 July 2009 as part of the MEGAPOLI experiment. The flight trajectory consisted of a loop around the Paris metropolis area and then a series of horizontal transects over the plume for a distance up to 200 km and at altitudes less than 700 m above sea level. RFs were carried out in the northerly, north-easterly, and easterly direction from the center of Paris depending on the wind directions. The aim of this flight plan was to measure the urban plume at several distances and at increasing oxidation time as it was leaving the Paris metropolitan area. PTR-MS data is available for a total of four flights and $\text{NO}_x / \text{NO}_y$ measurements are available for five RFs. A list of all measurements aboard the ATR-42 for each research flight is presented in Table S1.

3.1 General results for particle and gas-phase composition

Measurements of gas-phase species showed sharp increases in NO and NO_2 concentrations within the plume boundaries for each RF. Similar, but less pronounced increases were observed for CO. Ozone concentrations within the plume gradually increased with increasing distance from the city. Within the centre of the plume when

NO, NO₂, and NO_y concentrations are highest there are decreases in O₃ concentration (Fig. 2b), showing that O₃ is being rapidly consumed in the reaction:



Measured gas-phase species (NO_x/NO_y) are used as a proxy for the photochemical age of the air masses around Paris. In general, lower values of $-\log(\text{NO}_x/\text{NO}_y)$ represent air masses closer to the source and as the air-mass becomes more aged $-\log(\text{NO}_x/\text{NO}_y)$ approaches 1 (e.g. Kleinman et al., 2007). During the MEGAPOLI experiment, the measured in plume concentration of $-\log(\text{NO}_x/\text{NO}_y)$ only varied between 0.04 and 0.7 indicating that the measured air-masses were not very aged. This is expected since the aircraft only measured within 200 km from the centre of Paris, where as other airborne studies (MILAGRO) measured up to 600 km from the source area, and the subsequent $-\log(\text{NO}_x/\text{NO}_y)$ ranged from 0.1 to 1 (DeCarlo et al., 2008). VOC measurements show increases in measured concentrations of anthropogenic marker peaks (Toluene, Benzene, C8-aromatics) within the urban plume. However, biogenic marker peaks (isoprene) did not show peaks within the plume (Fig. S4). More details on the airborne VOC measurements during MEGAPOLI are described in Borbon et al. (2012).

RFs were classified based on the flight direction. Measured PM₁ mass concentrations (mass concentration measured by the C-ToF-AMS and BC mass concentrations) during each research flight were strongly dependent on the air mass trajectory and the residence time over land. Four of the northerly flights (N13, N16, N21, N29) and one of the northeasterly flights (NE28) were classified as highly polluted with highest average PM₁ mass concentrations within the plume ($6.3 \pm 3.3 \mu\text{g m}^{-3}$) and were dominated by organic compounds (> 50 %) (Figs. 2 and 3). Air-masses sampled during northerly flights arrived from a southerly direction and spent the majority of time over land. During northerly flights, wind speeds measured downtown Paris (site) at 40 m and 200 m using a mast were $3.78 \pm 0.53 \text{ m s}^{-1}$ and $6.36 \pm 1.9 \text{ m s}^{-1}$ respectively. All of these flights took place during days with no clouds and high temperatures (30 °C) where photochemical

Impact of urban emissions on regional aerosol particles

E. J. Freney et al.

Title Page

Abstract

Introduction

Conclusions

References

Tables

Figures

⏪

⏩

◀

▶

Back

Close

Full Screen / Esc

Printer-friendly Version

Interactive Discussion



Impact of urban emissions on regional aerosol particles

E. J. Freney et al.

Title Page

Abstract

Introduction

Conclusions

References

Tables

Figures

⏪

⏩

◀

▶

Back

Close

Full Screen / Esc

Printer-friendly Version

Interactive Discussion

mass concentration (f_{44}) against the contribution of m/z 43 to the total organic mass concentration (f_{43}) in a triangular space for each of the N research flights (Fig. 5) and for each of the E or NE flights (Fig. S5). F_{44} corresponds mainly to the oxidized mass fragment (CO_2^+) while f_{43} corresponds to a hydrocarbon fragment (C_3H_7^+). The black dotted lines show boundaries determined from a comparison of an ensemble of secondary organic aerosol measurements conducted in the northern hemisphere (Ng et al., 2010). In general, as the organic aerosol becomes more aged (oxidized), the f_{44} will become more important with all points approaching the top of the triangle. The fraction of f_{44} measured by the C-ToF-AMS is always less than 0.15 but more than 0.05 which is characteristic of semi- to low-volatile organic species. One exception to this was the N29 flight where the f_{44} of the aerosol was lower than the other northerly flights, showing a much less oxidized organic aerosol. In contrast to Ng et al. (2010) all organic aerosols (primary and secondary) are included.

Organic aerosol particles measured during each of the N flights have different and isolated properties based on the f_{44} vs. f_{43} signals. The E and NE flights, however, show organic aerosols with similar properties for each flight (Fig. S6). The two flights with the largest difference are N21 and N29. These two flights were both northerly sector flights and had BC values measured within the urban plume $> 0.9 \mu\text{g m}^{-3}$. Both flights had a high contribution of organics $> 45\%$. However, N21 ($\text{Org} = 6.5 \mu\text{g m}^{-3}$) had considerably higher background organic mass concentrations (and higher f_{44} values) than N29 ($\text{Org} = 1.9 \mu\text{g m}^{-3}$). The contributions from inorganic aerosols were similar (average inorganics $30\% \pm 5\%$). The maximum photochemical age of these flights determined using the value of $-\log(\text{NO}_x/\text{NO}_y)$ shows that the pollution measured during N21 is far more aged (0.63) than during N29 (0.35). Air mass back trajectories of N21 show that the air masses spent at least two days over SW France and Spain and likely picked up SOA there, which results in a higher organic aerosol background. Air masses arriving during N29 had the same origin but with a shorter continental residence time (Fig. 1). This results in a lower level of background aerosol and a much larger contribution from urban emissions within Paris and therefore a much less oxidized aerosol.

Impact of urban emissions on regional aerosol particles

E. J. Freney et al.

Title Page

Abstract

Introduction

Conclusions

References

Tables

Figures

⏪

⏩

◀

▶

Back

Close

Full Screen / Esc

Printer-friendly Version

Interactive Discussion



significant contributions from m/z 43 ($f_{43} = 0.09$) and from m/z 55 ($f_{55} = 0.08$) as well as m/z 57 ($f_{57} = 0.03$) (Figs. S6–S8) and correlated with the reference mass spectra for HOA (Ng et al., 2011), (Pearsons r (P_R) = 0.86) correlations with reference mass spectra of LV-OOA and of SV-OOA are less than $P_R = 0.45$. The temporal evolution of the HOA species correlated with primary particulate and gas-phase species such as BC ($P_R = 0.64 \pm 0.17$) and toluene ($P_R = 0.62 \pm 0.14$). The SV-OOA correlated with reference mass spectra SV-OOA and LV-OOA (Ng et al., 2011) ($P_R = 0.75$ and $P_R = 0.77$ respectively) and had contributions from m/z 43 ($f_{43} = 0.13$), m/z 44 ($f_{44} = 0.18$), and from m/z 55 ($f_{55} = 0.02$) (Figs. S6–S8). The SV-OOA species also correlated with primary marker species BC ($P_R = 0.50 \pm 0.11$) and toluene ($P_R = 0.44 \pm 0.14$). The LV-OOA had high contributions of m/z 44 ($f_{44} = 0.32$) and low contributions from primary marker peaks such as m/z 43 ($f_{43} = 0.09$) and m/z 55 ($f_{55} = 0.02$). In addition, it correlated well with reference mass spectra for LV-OOA ($P_R = 0.85$). Correlations with temporal evolution of SO_4 particles are low. This is expected since the majority of the SO_4 mass is measured outside of the urban plume boundaries and a large fraction of the organic aerosol is measured inside the urban plume boundaries.

The organic mass spectra were further explored with the ME-2 tool (Canonaco et al., 2013) by constraining the factor profiles of the primary species cooking and marine that has been modeled with ground based measurements during the same period of measurement (Crippa et al., 2013b). However, the time dependence of the marine factor was not correlated with the ground based data and the inclusion of cooking deteriorated the correlation of BC and HOA. Therefore, only the PMF solution with three factors is considered here.

3.2.2 Analysis of the organic build-up within the plume

Several studies (Volkamer et al., 2006; Kleinman et al., 2008; DeCarlo et al., 2010), have shown that the OA increases rapidly with the air mass photochemical age. During this study the photochemical age of the air masses is approximated using gas-phase measurements (NO_x/NO_y). NO_x/NO_y measurements were available during four RFs

Impact of urban emissions on regional aerosol particles

E. J. Freney et al.

Title Page

Abstract

Introduction

Conclusions

References

Tables

Figures

⏪

⏩

◀

▶

Back

Close

Full Screen / Esc

Printer-friendly Version

Interactive Discussion



(E20, N21, NE28, N29). Among these four flights, only two (N21 and N29) had simultaneous measurements of aerosol composition (C-ToF-AMS), VOCs (PTR-MS) (Table S1). When using NO_x and NO_y measurements as an indicator of photochemical age it is necessary to assure that there are not multiple sources of NO_x emissions that would result in an incorrect measurement of the photochemical age. During the MEGAPOLI experiment, increases in NO_y , NO_x and other gas-phase species were only observed within the plume boundaries. It is therefore assumed that the calculated photochemical age is representative of urban emissions from Paris, and that there are no nearby sources of pollution contributing to the increases in NO_y and NO_x observed during the measurement period (Figs. 2 and S2).

Aerosol measurements are most commonly normalized with measurements of CO. However, during our measurement period the difference between the background and local CO measurements were small and the absolute CO concentrations were low (< 150 ppb). For this reason, our initial calculations used BC to normalize aerosol measurements. As noted by Park et al. (2005), BC mixed with soluble aerosol particles could be susceptible to wet deposition. In good weather conditions, wet deposition is not likely to be important and the BC concentration should be conserved. Background values of Org, LV-OOA, SV-OOA, HOA, and BC were used to calculate the increase in the organic (ΔOrg) and BC (ΔBC) mass concentrations resulting from the urban plume.

Increases in OA (ΔOA) and NO_3 (ΔNO_3) above background are normalized to ΔBC . The ratios of $\Delta\text{OA}/\Delta\text{BC}$ and $\Delta\text{NO}_3/\Delta\text{BC}$ are then averaged over seven different subsets of photochemical age ranging from 0 to > 0.6 at intervals of 0.1. For each research flight we observe increases in $\Delta\text{OA}/\Delta\text{BC}$ with increasing $-\log(\text{NO}_x/\text{NO}_y)$. Average values for three flights gave an $r^2 = 0.95 \pm 0.04$ and slope = 1.11 ± 0.596 (Fig. S2d). In comparison, the $\Delta\text{NO}_3/\Delta\text{BC}$ shows little change as the photochemical age increases. These increases in OA so close to the source of the urban plume illustrates that OA is being formed from anthropogenic emissions from the Paris region. These observations are in agreement with recent studies by Chirico et al. (2010) and Platt et al. (2012) who demonstrated that SOA from diesel and gasoline vehicles are rapidly formed.

Impact of urban emissions on regional aerosol particles

E. J. Freney et al.

Title Page

Abstract

Introduction

Conclusions

References

Tables

Figures

⏪

⏩

◀

▶

Back

Close

Full Screen / Esc

Printer-friendly Version

Interactive Discussion



In order to examine how the different types of OA change as a function of photochemical age we compared the three OA aerosol types ($\Delta\text{LV-OOA}/\Delta\text{BC}$, $\Delta\text{SV-OOA}/\Delta\text{BC}$, and $\Delta\text{HOA}/\Delta\text{BC}$) with $-\log(\text{NO}_x/\text{NO}_y)$ values for the four flights; N16, E20, N21, and N29. The averaged ratio of $\Delta\text{LV-OOA}/\Delta\text{BC}$ and the $\Delta\text{SV-OOA}/\Delta\text{BC}$ for all flights showed increases by a factor of 2.12 and 1.98 respectively when the $-\log(\text{NO}_x/\text{NO}_y)$ increased from 0.1 up to 0.6, the $\Delta\text{HOA}/\Delta\text{BC}$ ratios only varied slightly with an average ratio of 1.28 (Fig. 6). These measurements show that the observed increase in OA as a function of photochemical age is predominantly composed of SOA.

3.2.3 Understanding the production of OA within the plume

Similar to previous studies (Kleinman et al., 2008) we attempt to apportion the increase in organic aerosol to certain types of aerosol sources. We first recalculate the increase in OA relative to CO rather than to BC, allowing us to compare with other studies and to compare with the formation of secondary organic aerosol resulting from gas-phase precursors. Unlike other studies our absolute CO emissions and the ratio of our local CO emissions to background CO emissions were very low, with local CO emissions only increasing by 30 and 60 ppb above the background. However, Fig. 7 illustrates that similar to the $\Delta\text{OA}/\Delta\text{BC}$, the $\Delta\text{OA}/\Delta\text{CO}$ ratio increases with photochemical age. The addition of OA to the plume as a result of aging was calculated using Eq. (5):

$$(\Delta\text{OA}/\Delta\text{CO}) = (\Delta\text{OA}/\Delta\text{CO})_{(X)} - (\Delta\text{OA}/\Delta\text{CO})_{(Y)}. \quad (5)$$

where X and Y represents the photochemical age furthest from the source and nearest to the source, respectively. Using this Eq. (5), we calculated $\Delta\text{OA}/\Delta\text{CO}$ of 70, 69, 72, and $65 \mu\text{g m}^{-3} \text{ppm}^{-1}$ CO for N16, N20, N21, and N29 using a maximum value of $-\log(\text{NO}_x/\text{NO}_y)$ of 0.6, 0.3, 0.7, and 0.3, respectively (Table 3). Assuming that all the organic mass added during photochemical aging is OOA (Oxidised organic aerosol) with a carbon content, OC we can use the ratio $\text{OOA}/\text{OC} = 2.2 \mu\text{g} \mu\text{gC}^{-1}$ (Zhang et al., 2005). Therefore the carbon added to the aerosol phase during photochemical aging is 31.8, 31.3, 32.7, and $29.5 \mu\text{gC m}^{-3} \text{ppm CO}^{-1}$ for N16, N20, N21, and N29.

Impact of urban emissions on regional aerosol particles

E. J. Freney et al.

Title Page

Abstract

Introduction

Conclusions

References

Tables

Figures

⏪

⏩

◀

▶

Back

Close

Full Screen / Esc

Printer-friendly Version

Interactive Discussion

These values are very similar to those of Kleinman et al. (2008 and 2007) (Table 3) even though there are large differences in the absolute CO values observed. CO concentrations measured during MEGAPOLI (150 ppb) are much lower than those measured in both the New England, USA (325 ppb) and in Mexico city (> 500 ppb). In addition to variations in the sources and emissions from region to region (Mexico city and Paris), each of the RFs during MEGAPOLI were exposed to air masses with different histories. RF N21 and N29 are both influenced by southerly air masses, however, air mass for N21 had spent long periods of time over southern France and had much higher background OA concentrations than N29. Air masses for N29 spent much less time over land and the background OA was lower. This is also observed in Table 3 where values of $\Delta\text{OA}/\Delta\text{CO}$ near the source and after aging are higher for N21 than for N29. As noted by Kleinman et al. (2008), it is not known how CO emission sources change from region to region and therefore the $\Delta\text{OA}/\Delta\text{CO}$ $\mu\text{g m}^{-3}$ ppm^{-1} CO may not be comparable between studies. However, Table 3 shows that the absolute concentrations of CO emissions do not have an impact on the production of OA per unit of CO.

As already mentioned in Sect. 2.3, care must be taken when defining background values of OA and CO. For example, for E16, the background value of CO was chosen to be 87 ppb. This was calculated by averaging CO measurements outside of the plume, in the same way as was done for BC and OA (Sect. 2.3). If we increase this background to 97 ppb, the $\Delta\text{OA}/\Delta\text{CO}$ $\mu\text{g m}^{-3}/\text{ppm}$ CO increases from 70 to 110. If the background CO is decreased to 77 ppb the $\Delta\text{OA}/\Delta\text{CO}$ $\mu\text{g m}^{-3}/\text{ppm}$ CO decreases to 34. In addition to uncertainties associated with the determination of background values, it is necessary to account for different photochemical ages among the different research flights and among different studies. In the studies in the New England, USA and in Mexico city the photochemical ages ($-\log(\text{NO}_x/\text{NO}_y)$) ranged from 0 up to 0.94, however the maximum photochemical ages measured within the plume during this study varied from low values of 0.3 (E20 and N29) up to 0.7 (N16 and N21).

Despite uncertainties in the measurements, the similarities within our results and those from other regions, highlights the importance of having simultaneous gas and particle phase measurements available during studies in order to put the formation and aging of secondary organic aerosol particles in the atmosphere into the perspective of emissions.

3.2.4 Sources of organic aerosol particles within the plume

A number of field studies have shown that in the atmosphere rapid increases in the formation of SOA were linked to the oxidation of anthropogenic VOCs (Volkamer et al., 2006). The use of C8-aromatics/CO ratio is another proxy of photochemical depletion by anthropogenic VOCs occurring within the Paris plume. Borbon et al. (2013) shows that C8-aromatics concentrations decreased faster than CO at the timescale of the Paris plume transport compared to benzene and toluene. This ratio is therefore expected to decrease as photochemical age ($-\log(\text{NO}_x/\text{NO}_y)$) increases as revealed when coloring Figs. 1d and 2d (Figs. S1d and S2d) by the ratio of C8-aromatics/CO. This pattern together with measurements showing increases in typical anthropogenic VOC marker peaks within the plume (m/z 93 (Toluene) $\Delta\text{Toluene}_{\text{PLUME}}/\text{Toluene}_{\text{BKG}} = 109 \pm 40\%$, m/z 79 (Benzene) $90 \pm 40\%$ $\Delta\text{Benzene}_{\text{PLUME}}/\text{Benzene}_{\text{BKG}}$, Fig. S4) suggests that anthropogenic VOC emissions are most likely contributing to the formation of SOA within the plume. Biogenic marker peaks, such as isoprene, did not show significant increases within the plume (Fig. S4) ($\Delta\text{Isoprene}_{\text{PLUME}}/\text{Isoprene}_{\text{BKG}} = -5 \pm 5\%$).

PTRMS VOC measurements were only available for N21 and N29. Using these measurements we attempt to estimate the yield of OA that would be produced from the available gas-phase precursors using Eq. (6) for N21 and N29.

$$\left(\frac{\Delta\text{OA}}{\Delta\text{CO}}\right)_{\text{predicted}} = \left(\frac{\sum \text{ppb C}\Delta\text{HC}_i}{\text{ppmv}\Delta\text{CO}}\right) \quad (6)$$

H*C*_{*i*} corresponds to the each VOC species used. For benzene and toluene we used yields reported by Ng et al. (2007) for low values of NO_x and ΔHC_{*i*}, to calculate the

24904

Impact of urban emissions on regional aerosol particles

E. J. Freney et al.

Title Page

Abstract

Introduction

Conclusions

References

Tables

Figures

⏪

⏩

◀

▶

Back

Close

Full Screen / Esc

Printer-friendly Version

Interactive Discussion



Impact of urban emissions on regional aerosol particles

E. J. Freney et al.

Title Page

Abstract

Introduction

Conclusions

References

Tables

Figures

⏪

⏩

◀

▶

Back

Close

Full Screen / Esc

Printer-friendly Version

Interactive Discussion

aerosol formation from the measured aromatics aboard the ATR-42. For the sum of C8-aromatics and C9-aromatics (Table S4), we used the yield value of m-xylene from Ng et al. (2007). Biogenic VOCs were not included in this calculation. The calculated yields result in 80 ± 3 ppbC per ppm CO and 32.3 ± 3.2 ppbC per ppm CO for N21 and N29, respectively. Predicted values are higher than the 65.4 ppbC per ppm measured for N21 (Sect. 3.2.3), and represent 54 % of the measured 59 ppbC per ppm for N29. Higher values in N21 may be related to the sparse data points available for N21 (Fig. S2). The values of SOA yield are strongly dependent on laboratory conditions. In addition to NO_x levels, SOA yield values are also proportional to the concentrations of total organic carbon which is usually much higher than its corresponding ambient levels. Therefore, the estimation of the SOA yields rather provides a sense of the potential impact of anthropogenic VOCs on SOA production within the plume. If we calculate the amount of OA in the plume using the high NO_x yields reported in Ng et al. (2007), similar to those used by Kleinman et al. (2008), our estimated yield of $\Delta\text{OA} / \Delta\text{CO}$ drops to 23 and 9.7 ppbC per ppm CO, representing only 35 % and 15 ± 1 % of the measured $\Delta\text{OA} / \Delta\text{CO}$. This may partly explains why such a small fraction of the organic mass was accounted for by anthropogenic VOCs in Kleinman et al. (2008) and demonstrates the importance of improving our knowledge of secondary organic aerosol formation processes through controlled laboratory measurements. For this calculation, we only consider the available on board measurements of benzene, toluene, C8-aromatics and C9-aromatics (Aït-Helal et al., 2013). Although, recent observations by Shilling et al. (2013) demonstrated the importance of the combined biogenic and anthropogenic emissions on the formation of OA, the similar concentrations of isoprene measured within and outside of the Paris urban plume do not suggest stronger biogenic secondary OA within the plume compared to outside.

4 Summary

Measurements aboard the ATR-42 during the MEGAPOLI experiment in July 2009 have allowed us to study the composition and evolution of aerosol particle and gas-phase species as urban emissions leave Paris. Each RF was performed over a relatively small geographical area (< 200 km) allowing rapid changes in aerosol mass concentration to be monitored.

Similar to observations made by Freutel et al. (2013) we observe that largest differences in aerosol concentration and BC levels are related mainly to air-mass origin. Air-masses that had spent most time over land had higher levels of BC, organic, and nitrate concentrations than westerly air-masses that spent less time over land. Northerly sector flights contain the highest fractions of organic aerosol particles and highest BC concentrations whereas easterly sector flights had lower aerosol mass concentrations. The composition of the urban plume (ΔC) can be described by high contributions of organic (N = 48 %, E/NE = 54 %), BC (N = 22 %, E/NE = 15 %), and NO_3 (N = 17 %, E/NE = 19 %) particles.

Organic aerosol particles normalized to BC increased as a function of photochemical age. The plotted ratios of PMF resolved OA ($\Delta LV\text{-}OOA/\Delta BC$, $\Delta SV\text{-}OOA/\Delta BC$, and $\Delta HOA/\Delta BC$) as a function of photochemical age ($-\log(NO_x/NO_y)$) show that increases in OA is dominated by secondary OA species.

At the ground based site Freutel et al. (2013), did not observe a significant increase in OOA at three different measurement sites within Paris and concluded that the majority of the OOA missions were linked to regional emissions rather than local emissions. Similar findings were reported during the REPARTEE campaign in London (Harrison et al., 2012). However, the increase of $\Delta OA/\Delta CO$ with photochemical age measured aboard the ATR-42, demonstrates that it is necessary to take into account a larger geographical area when assessing the formation of SOA from urban emissions.

Simultaneous AMS, NO_x/NO_y and VOC measurements were available during two research flights. Using only four anthropogenic marker species and organic aerosol

Impact of urban emissions on regional aerosol particles

E. J. Freney et al.

Title Page

Abstract

Introduction

Conclusions

References

Tables

Figures



Back

Close

Full Screen / Esc

Printer-friendly Version

Interactive Discussion

formation yields reported for low NO_x conditions we were able to predict ~ 50 % of the organic aerosol measured in the plume. This good agreement between predicted and measured values is a result of the improved knowledge of aerosol formation properties from laboratory studies on gas-to-particle reaction processes.

The magnitude of the increase $\Delta\text{OA}/\Delta\text{CO}$ measured during MEGAPOLI is similar for flights exposed to air masses with different source regions and compare well with equivalent measurements from other studies in Mexico city and in the New England, USA. These results confirm previous observations of Kleinman et al. (2008) stating that aerosol yields remain similar regardless of the level of pollution.

Supplementary material related to this article is available online at <http://www.atmos-chem-phys-discuss.net/13/24885/2013/acpd-13-24885-2013-supplement.pdf>.

Acknowledgements. We would like to thank all the pilots and flight crew from SAFIRE for their help and enthusiasm. We gratefully acknowledge the European Union's Seventh Framework Programme FP/2007–2011 within the project MEGAPOLI (grant agreement no. 212520) for supporting the field experiments. E. Freney would also like to acknowledge the AXA research fund and the Marie Curie reintegration grant (grant agreement no. 276728) for postdoctoral research funds.



The publication of this article is financed by CNRS-INSU.

Impact of urban emissions on regional aerosol particles

E. J. Freney et al.

Title Page

Abstract

Introduction

Conclusions

References

Tables

Figures

⏪

⏩

◀

▶

Back

Close

Full Screen / Esc

Printer-friendly Version

Interactive Discussion



References

- Ait-Helal, W., Borbon A., Sauvage, S., De Gouw, J. A., Colomb A., Beekmann, M., Afif, C., Durand-Jolibois, R., Fronval, I., Grand, N., Leonardis, T., Michoud V., Miet K., Perrier, S., Siour, G., Zapf, P., Doussin, J. F., Lopez, M., Gros, V., Freutel, F., Schneider, J., Crippa, M., Prevot, A. S. H., Baltensperger, U., and Locoge, N.: I/VOC in sub-urban Paris: variability, origin and importance in SOA formation, *Atmos. Chem. Phys. Discuss.*, in preparation, 2012.
- Allan, J. D., Delia, A. E., Coe, H., Bower, K. N., Alfarra, M. R., Jimenez, J. L., Middlebrook, A. M., Drewnick, F., Onasch, T. B., Canagaratna, M. R., Jayne, J. T., and Worsnop, D. R: A generalised method for the extraction of chemically resolved mass spectra from aerodyne aerosol mass spectrometer data, *J. Aerosol. Sci.*, 35, 909–922, 2004.
- Atkinson, R. and Arey, J.: Atmospheric degradation of volatile organic compounds, *Chem. Rev.*, 103, 4605–4638, 2003.
- Bahrieni, R., Dunlea, E. J., Matthew, B. M., Simons, C., Docherty, K. S., Carlo, P. F., Jimenez, J. L., Brock, C. A., and Middlebrook, A. M.: Design and operation of a pressure-controlled inlet for airborne sampling with an aerodynamic aerosol lens, *Aerosol Sci. Tech.*, 42, 465–471, doi:10.1080/02786820802178514, 2008.
- Bahrieni, R., Middlebrook, A. M., de Gouw, J. A., Warneke, C., Trainer, M., Brock, C. A., Stark, H., Brown S. S., Dube, W. P., Gilman, J. B., Hall, K., Holloway, J. S., Kuster, W. C., Perring, A. E., Prevot, A. S. H., Schwarz, J. P., Spackman, J. R., Szidat, S., Wagner, N. L., Weber, R. J., Zotter, P., and Parrish, D. D.: Gasoline emissions dominate over diesel in formation of secondary organic aerosols mass, *Geophys. Res. Lett.*, 39, L06805, doi:10.1029/2011GL050718, in press, 2012.
- Baklanov, A., Lawrence, M., Pandis, S., Mahura, A., Finardi, S., Moussiopoulos, N., Beekmann, M., Laj, P., Gomes, L., Jaffrezo, J.-L., Borbon, A., Coll, I., Gros, V., Sciare, J., Kukkonen, J., Galmarini, S., Giorgi, F., Grimmond, S., Esau, I., Stohl, A., Denby, B., Wagner, T., Butler, T., Baltensperger, U., Buitjes, P., van den Hout, D., van der Gon, H. D., Collins, B., Schluenzen, H., Kulmala, M., Zilitinkevich, S., Sokhi, R., Friedrich, R., Theloke, J., Kummer, U., Jalkinen, L., Halenka, T., Wiedensholer, A., Pyle, J., and Rossow, W. B.: MEGAPOLI: concept of multi-scale modelling of megacity impact on air quality and climate, *Adv. Sci. Res.*, 4, 115–120, doi:10.5194/asr-4-115-2010, 2010.
- Borbon, A., Gilman, J. B., Kuster, W. C., Grand, N., Chevaillier, S., Colomb1, A., Dolgorouky, C., Gros, V., Lopez, M., Sarda-Esteve, R., Holloway, J., Stutz, J., Atkin K., Perrussel, O.,

Impact of urban emissions on regional aerosol particles

E. J. Freney et al.

Title Page

Abstract

Introduction

Conclusions

References

Tables

Figures



Back

Close

Full Screen / Esc

Printer-friendly Version

Interactive Discussion



Impact of urban emissions on regional aerosol particles

E. J. Freney et al.

Title Page

Abstract

Introduction

Conclusions

References

Tables

Figures

◀

▶

◀

▶

Back

Close

Full Screen / Esc

Printer-friendly Version

Interactive Discussion

atmosphere: Results from the New England Air Quality Study in 2002, *J. Geophys. Res.-Atmos.*, 110, D16305, doi:10.1029/2004JD005623, 2005.

DeCarlo, P. F., Dunlea, E. J., Kimmel, J. R., Aiken, A. C., Sueper, D., Crounse, J., Wennberg, P. O., Emmons, L., Shinozuka, Y., Clarke, A., Zhou, J., Tomlinson, J., Collins, D. R., Knapp, D., Weinheimer, A. J., Montzka, D. D., Campos, T., and Jimenez, J. L.: Fast airborne aerosol size and chemistry measurements above Mexico City and Central Mexico during the MILAGRO campaign, *Atmos. Chem. Phys.*, 8, 4027–4048, doi:10.5194/acp-8-4027-2008, 2008.

DeCarlo, P. F., Ulbrich, I. M., Crounse, J., de Foy, B., Dunlea, E. J., Aiken, A. C., Knapp, D., Weinheimer, A. J., Campos, T., Wennberg, P. O., and Jimenez, J. L.: Investigation of the sources and processing of organic aerosol over the Central Mexican Plateau from aircraft measurements during MILAGRO, *Atmos. Chem. Phys.*, 10, 5257–5280, doi:10.5194/acp-10-5257-2010, 2010.

Docherty, K. S., Aiken, A. C., Huffman, J. A., Ulbrich, I. M., DeCarlo, P. F., Sueper, D., Worsnop, D. R., Snyder, D. C., Peltier, R. E., Weber, R. J., Grover, B. D., Eatough, D. J., Williams, B. J., Goldstein, A. H., Ziemann, P. J., and Jimenez, J. L.: The 2005 Study of Organic Aerosols at Riverside (SOAR-1): instrumental intercomparisons and fine particle composition, *Atmos. Chem. Phys.*, 11, 12387–12420, doi:10.5194/acp-11-12387-2011, 2011.

Drewnick, F., Hings, S. S., DeCarlo, P. F., Jayne, J. T., Gonin, M., Fuhrer, K., Weimer, S., Jimenez, J. L., Demerjian, K. L., Borrmann, S., and Worsnop, D. R.: A new Time-of-Flight Aerosol Mass Spectrometer (ToF-AMS) – Instrument Description and First Field Deployment. *Aerosol Sci. Tech.*, 39, 637–658, 2005.

Freney, E. J., Sellegri, K., Canonaco, F., Boulon, J., Hervo, M., Weigel, R., Pichon, J. M., Colomb, A., Prévôt, A. S. H., and Laj, P.: Seasonal variations in aerosol particle composition at the puy-de-Dôme research station in France, *Atmos. Chem. Phys.*, 11, 13047–13059, doi:10.5194/acp-11-13047-2011, 2011.

Freutel, F., Schneider, J., Drewnick, F., von der Weiden-Reinmüller, S.-L., Crippa, M., Prévôt, A. S. H., Baltensperger, U., Poulain, L., Wiedensohler, A., Sciare, J., Sarda-Estève, R., Burkhardt, J. F., Eckhardt, S., Stohl, A., Gros, V., Colomb, A., Michoud, V., Doussin, J. F., Borbon, A., Haeffelin, M., Morille, Y., Beekmann, M., and Borrmann, S.: Aerosol particle measurements at three stationary sites in the megacity of Paris during summer 2009: meteorology and air mass origin dominate aerosol particle composition and size distribution, *Atmos. Chem. Phys.*, 13, 933–959, doi:10.5194/acp-13-933-2013, 2013.

Impact of urban emissions on regional aerosol particles

E. J. Freney et al.

Title Page

Abstract

Introduction

Conclusions

References

Tables

Figures

◀

▶

◀

▶

Back

Close

Full Screen / Esc

Printer-friendly Version

Interactive Discussion

Healy, R. M., Sciare, J., Poulain, L., Kamili, K., Merkel, M., Müller, T., Wiedensohler, A., Eckhardt, S., Stohl, A., Sarda-Estève, R., McGillicuddy, E., O'Connor, I. P., Sodeau, J. R., and Wenger, J. C.: Sources and mixing state of size-resolved elemental carbon particles in a European megacity: Paris, *Atmos. Chem. Phys.*, 12, 1681–1700, doi:10.5194/acp-12-1681-2012, 2012.

Hodzic A., Vautard, R., Bessagnet, B., Lattuati, M., and Moreto F.: Long-term urban aerosol simulation versus routine particulate matter observations, *Atmos. Environ.*, 39, 5851–5864, 2005.

Hodzic, A., Jimenez, J. L., Madronich, S., Canagaratna, M. R., DeCarlo, P. F., Kleinman, L., and Fast, J.: Modeling organic aerosols in a megacity: potential contribution of semi-volatile and intermediate volatility primary organic compounds to secondary organic aerosol formation, *Atmos. Chem. Phys.*, 10, 5491–5514, doi:10.5194/acp-10-5491-2010, 2010.

Kleinman, L. I., Springston, S. R., Daum, P. H., Lee, Y.-N., Nunnermacker, L. J., Senum, G. I., Wang, J., Weinstein-Lloyd, J., Alexander, M. L., Hubbe, J., Ortega, J., Canagaratna, M. R., and Jayne, J.: The time evolution of aerosol composition over the Mexico City plateau, *Atmos. Chem. Phys.*, 8, 1559–1575, doi:10.5194/acp-8-1559-2008, 2008.

Kleinman, L. I., Springston, S. R., Wang, J., Daum, P. H., Lee, Y.-N., Nunnermacker, L. J., Senum, G. I., Weinstein-Lloyd, J., Alexander, M. L., Hubbe, J., Ortega, J., Zaveri, R. A., Canagaratna, M. R., and Jayne, J.: The time evolution of aerosol size distribution over the Mexico City plateau, *Atmos. Chem. Phys.*, 9, 4261–4278, doi:10.5194/acp-9-4261-2009, 2009.

Lanz, V. A., Alfara, M. R., Baltensperger, U., Buchmann, B., Hueglin, C., and Prévôt, A. S. H.: Source apportionment of submicron organic aerosols at an urban site by factor analytical modelling of aerosol mass spectra, *Atmos. Chem. Phys.*, 7, 1503–1522, doi:10.5194/acp-7-1503-2007, 2007.

McMeeking, G. R., Bart, M., Chazette, P., Haywood, J. M., Hopkins, J. R., McQuaid, J. B., Morgan, W. T., Raut, J.-C., Ryder, C. L., Savage, N., Turnbull, K., and Coe, H.: Airborne measurements of trace gases and aerosols over the London metropolitan region, *Atmos. Chem. Phys.*, 12, 5163–5187, doi:10.5194/acp-12-5163-2012, 2012.

Middlebrook, A. M., Bahreini, R., Jimenez, J. L., and Canagaratna, M. R.: Evaluation of Composition-Dependent Collection Efficiencies for the Aerodyne Aerosol Mass Spectrometer using Field Data. *Aerosol Sci. Tech.*, 46, 258–271, doi:10.1080/02786826.2011.620041, 2012.

Impact of urban emissions on regional aerosol particles

E. J. Freney et al.

Title Page

Abstract

Introduction

Conclusions

References

Tables

Figures

◀

▶

◀

▶

Back

Close

Full Screen / Esc

Printer-friendly Version

Interactive Discussion

Nedelec, P., Cammas, J.-P., Thouret, V., Athier, G., Cousin, J.-M., Legrand, C., Abonnel, C., Lecoœur, F., Cayez, G., and Marizy, C.: An improved infrared carbon monoxide analyser for routine measurements aboard commercial Airbus aircraft: technical validation and first scientific results of the MOZAIC III programme, *Atmos. Chem. Phys.*, 3, 1551–1564, doi:10.5194/acp-3-1551-2003, 2003.

Ng, N. L., Chhabra, P. S., Chan, A. W. H., Surratt, J. D., Kroll, J. H., Kwan, A. J., McCabe, D. C., Wennberg, P. O., Sorooshian, A., Murphy, S. M., Dalleska, N. F., Flagan, R. C., and Seinfeld, J. H.: Effect of NO_x level on secondary organic aerosol (SOA) formation from the photooxidation of terpenes, *Atmos. Chem. Phys.*, 7, 5159–5174, doi:10.5194/acp-7-5159-2007, 2007.

Ng, N. L., Canagaratna, M. R., Zhang, Q., Jimenez, J. L., Tian, J., Ulbrich, I. M., Kroll, J. H., Docherty, K. S., Chhabra, P. S., Bahreini, R., Murphy, S. M., Seinfeld, J. H., Hildebrandt, L., Donahue, N. M., DeCarlo, P. F., Lanz, V. A., Prévôt, A. S. H., Dinar, E., Rudich, Y., and Worsnop, D. R.: Organic aerosol components observed in Northern Hemispheric datasets from Aerosol Mass Spectrometry, *Atmos. Chem. Phys.*, 10, 4625–4641, doi:10.5194/acp-10-4625-2010, 2010.

Ng, N. L., Canagaratna, M. R., Jimenez, J. L., Zhang, Q., Ulbrich, I. M., and Worsnop, D. R.: Real-Time Methods for Estimating Organic Component Mass Concentrations from Aerosol Mass Spectrometer Data, *Environ. Sci. Technol.*, 45, 910–916, doi:10.1021/es102951k, 2011.

Odum, J. R., Hoffman, T., Bowman, F., Collins, D., Flagan, R. C., and Seinfeld, J. H.: Gas/Particle partitioning and secondary organic aerosol yields, *Environ. Sci. Technol.*, 30, 2580–2585, 1996.

Paatero, P.: Least squares formulation of robust non-negative factor analysis, *Chemometr. Intell. Lab.*, 37, 23–35, 1997.

Paatero, P. and Tapper, U.: Positive matrix factorization – a nonnegative factor model with optimal utilization of error-estimates of data values, *Environmetrics*, 5, 111–126, 1994.

Park, R. J., Jacob, D. J., Palmer, P. I., Clarke, A. D., Weber, R. J., Zondlo, M. A., Eisele, F. L., Brandy, A. R., Thornton, D. C., Sachse, G. W., and Bond, T. C.: Export efficiency of black carbon aerosol in continental outflow: Global implications, *J. Geophys. Res.-Atmos.*, 110, D11205, doi:10.1029/2004JD005432, 2005.

Platt, S. M., El Haddad, I., Zardini, A. A., Clairrotte, M., Astorga, C., Wolf, R., Slowik, J. G., Temime-Roussel, B., Marchand, N., Ježek, I., Drinovec, L., Moc(nik, G., Möhler, O., Richter,

Impact of urban emissions on regional aerosol particles

E. J. Freney et al.

Title Page

Abstract

Introduction

Conclusions

References

Tables

Figures

⏪

⏩

◀

▶

Back

Close

Full Screen / Esc

Printer-friendly Version

Interactive Discussion

- R., Barmet, P., Bianchi, F., Baltensperger, U., and Prévôt, A. S. H.: Secondary organic aerosol formation from gasoline vehicle emissions in a new mobile environmental reaction chamber, *Atmos. Chem. Phys. Discuss.*, 12, 28343–28383, doi:10.5194/acpd-12-28343-2012, 2012.
- 5 Salcedo, D., Onasch, T. B., Aiken, A. C., Williams, L. R., de Foy, B., Cubison, M. J., Worsnop, D. R., Molina, L. T., and Jimenez, J. L.: Determination of particulate lead using aerosol mass spectrometry: MILAGRO/MCMA-2006 observations, *Atmos. Chem. Phys.*, 10, 5371–5389, doi:10.5194/acp-10-5371-2010, 2010.
- Sciare, J., d'Argouges, O., Zhang, Q. J., Sarda-Estève, R., Gaimoz, C., Gros, V., Beekmann, M., and Sanchez, O.: Comparison between simulated and observed chemical composition of fine aerosols in Paris (France) during springtime: contribution of regional versus continental emissions, *Atmos. Chem. Phys.*, 10, 11987–12004, doi:10.5194/acp-10-11987-2010, 2010.
- 10 Shilling, J. E., Zaveri, R. A., Fast, J. D., Kleinman, L., Alexander, M. L., Canagaratna, M. R., Fortner, E., Hubbe, J. M., Jayne, J. T., Sedlacek, A., Setyan, A., Springston, S., Worsnop, D. R., and Zhang, Q.: Enhanced SOA formation from mixed anthropogenic and biogenic emissions during the CARES campaign, *Atmos. Chem. Phys.*, 13, 2091–2113, doi:10.5194/acp-13-2091-2013, 2013.
- 15 Ulbrich, I. M., Canagaratna, M. R., Zhang, Q., Worsnop, D. R., and Jimenez, J. L.: Interpretation of organic components from Positive Matrix Factorization of aerosol mass spectrometric data, *Atmos. Chem. Phys.*, 9, 2891–2918, doi:10.5194/acp-9-2891-2009, 2009.
- 20 Volkamer, R., Jimenez, J. L., San Martini, F., Dzepina, K., Zhang, Q., Salcedo, D., Molina, L. T., Worsnop, D. R., and Molina, M. J.: Secondary organic aerosol formation from anthropogenic air pollution: Rapid and higher than expected, *Geophys. Res. Lett.*, 33, L17811, doi:10.1029/2006GL026899, 2006.
- Zhang, Q., Worsnop, D. R., Canagaratna M. R., and Jimenez, J. L.: Hydrocarbon-like and oxygenated organic aerosols in Pittsburgh: Insights into sources and processes or organic aerosol, *Atmos. Chem. Phys.*, 5, 3289–3311, 2005, <http://www.atmos-chem-phys.net/5/3289/2005/>.
- 25 Zhang, Q. J., Beekmann, M., Drewnick, F., Freutel, F., Schneider, J., Crippa, M., Prévôt, A. S. H., Baltensperger, U., Poulain, L., Wiedensohler, A., Sciare, J., Gros, V., Borbon, A., Colomb, A., Michoud, V., Doussin, J.-F., Denier van der Gon, H. A. C., Haeffelin, M., Dupont, J.-C., Siour, G., Petetin, H., Bessagnet, B., Pandis, S. N., Hodzic, A., Sanchez, O., Honoré, C., and Perrussel, O.: Formation of organic aerosol in the Paris region during the MEGAPOLI sum-
- 30

Impact of urban emissions on regional aerosol particles

E. J. Freney et al.

Title Page

Abstract

Introduction

Conclusions

References

Tables

Figures



Back

Close

Full Screen / Esc

Printer-friendly Version

Interactive Discussion

Impact of urban emissions on regional aerosol particles

E. J. Freney et al.

Title Page

Abstract

Introduction

Conclusions

References

Tables

Figures

⏪

⏩

◀

▶

Back

Close

Full Screen / Esc

Printer-friendly Version

Interactive Discussion

Table 1. Research flight number, date and principal measurements available during each flight. Total aerosol concentrations inside and outside the urban plume, percentage of organic contribution and mass concentrations of BC measured within the plume.

RF	Date	Mass concentration		Org %	BC	Flight sector	Flight classification
		Plume	Backgrd	($\mu\text{g m}^{-3}$)			
28	13/07/09	3.36	2.69	47	0.54	N	N13
29	15/07/09	3.21	2.41	40	0.28	NE	NE15
30	16/07/09	5.85	4.37	55	0.79	N	N16
31	20/07/09	7.34	6.61	45	0.40	E	E20
32	21/07/09	10.9	8.80	75	1.04	N	N21
33	25/07/09	4.18	3.16	33	0.28	E	E25
35	28/07/09	6.93	4.52	55	0.62	NE	NE28
36	29/07/09	3.02	2.89	65	0.94	N	N29

Impact of urban emissions on regional aerosol particles

E. J. Freney et al.

Title Page

Abstract

Introduction

Conclusions

References

Tables

Figures

◀

▶

◀

▶

Back

Close

Full Screen / Esc

Printer-friendly Version

Interactive Discussion

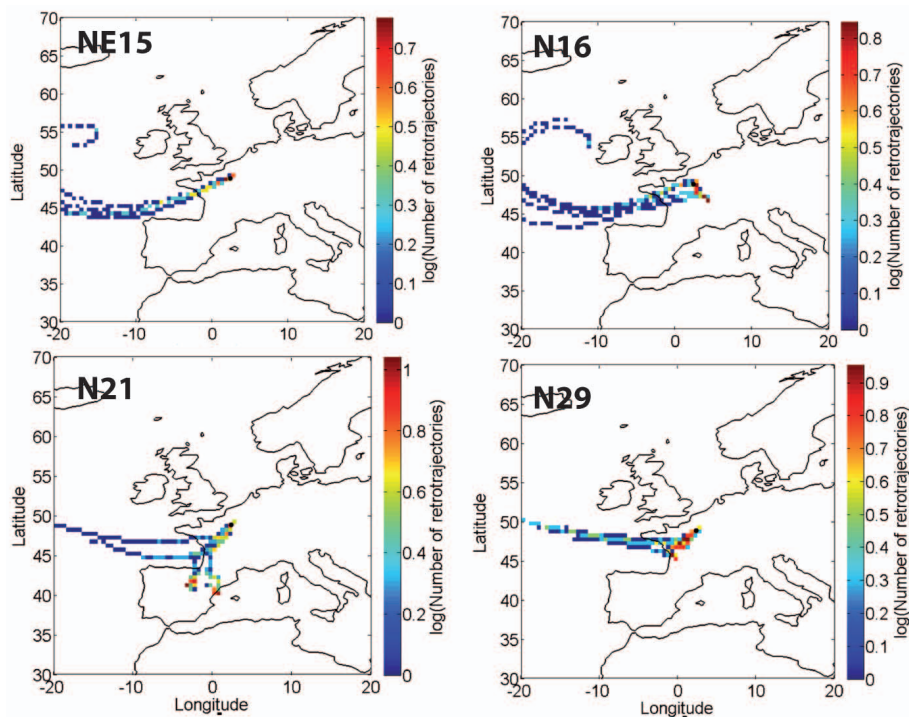


Fig. 1. Air mass backward trajectories calculated using HYSPLIT for 72 h. HYSPLIT trajectories are calculated at a height of 700 m in the hysplit model.

Impact of urban emissions on regional aerosol particles

E. J. Freney et al.

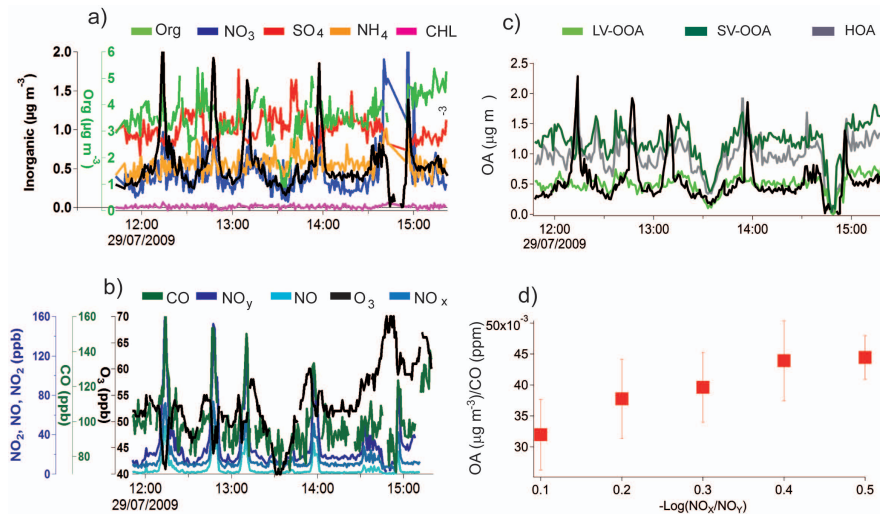


Fig. 2. An overview of aerosol gas and particle composition measured during N29. **(a)** Time series of AMS particle composition, and BC (in black). **(b)** Time series of gas-phase measurements, **(c)** PMF analysis of the organic aerosol mass spectra with BC, and **(d)** increase in the normalized organic aerosol mass concentration as a function of photochemical age.

Impact of urban emissions on regional aerosol particles

E. J. Freney et al.

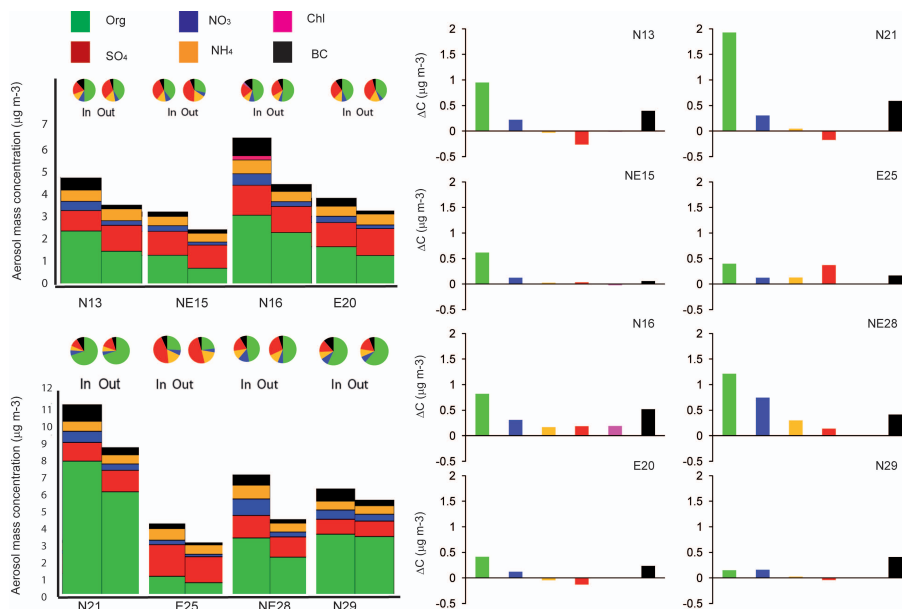


Fig. 3. The left hand side of the figure shows the aerosol composition measured inside and outside of the plume during each research flight. On the right hand side the average difference in composition (ΔC) between the inside and the outside of the urban plume for each flight is shown.

Title Page

Abstract Introduction

Conclusions References

Tables Figures

⏪ ⏩

⏴ ⏵

Back Close

Full Screen / Esc

Printer-friendly Version

Interactive Discussion



Impact of urban emissions on regional aerosol particles

E. J. Freney et al.

Title Page

Abstract

Introduction

Conclusions

References

Tables

Figures

◀

▶

◀

▶

Back

Close

Full Screen / Esc

Printer-friendly Version

Interactive Discussion

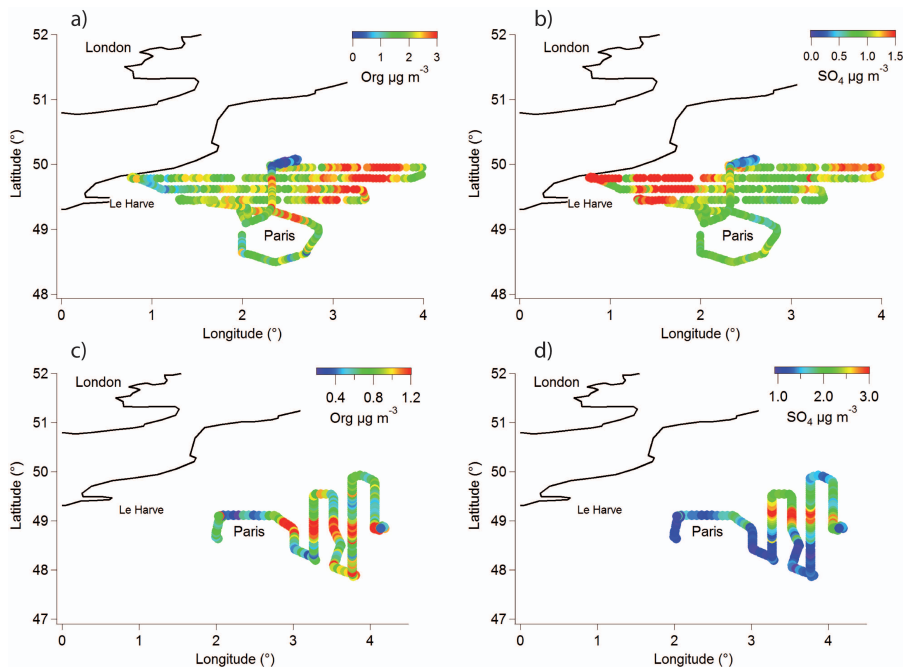


Fig. 4. Flight tracks around the Paris region for N13 (a, b) and E25 (c, d) colored by SO_4 (b, c) and Org (a, c).

Impact of urban emissions on regional aerosol particles

E. J. Freney et al.

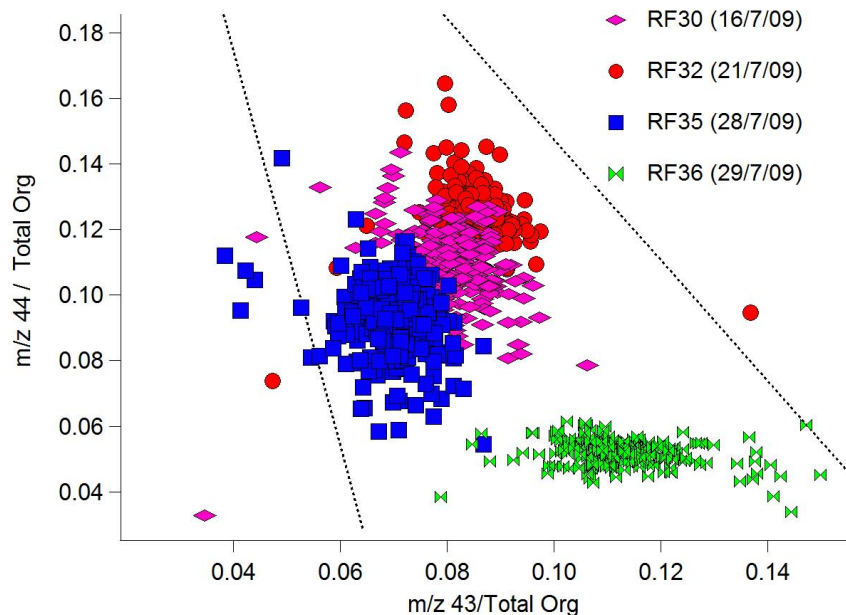


Fig. 5. Fraction of Org44 to total Organics (f_{44}) against the fraction of Org 43 to total Organics (f_{43}) for N16, N21, NE28, and N29. The black dotted lines show boundaries set by Ng et al. (2010).

[Title Page](#)[Abstract](#)[Introduction](#)[Conclusions](#)[References](#)[Tables](#)[Figures](#)[⏪](#)[⏩](#)[⏴](#)[⏵](#)[Back](#)[Close](#)[Full Screen / Esc](#)[Printer-friendly Version](#)[Interactive Discussion](#)

Impact of urban emissions on regional aerosol particles

E. J. Freney et al.

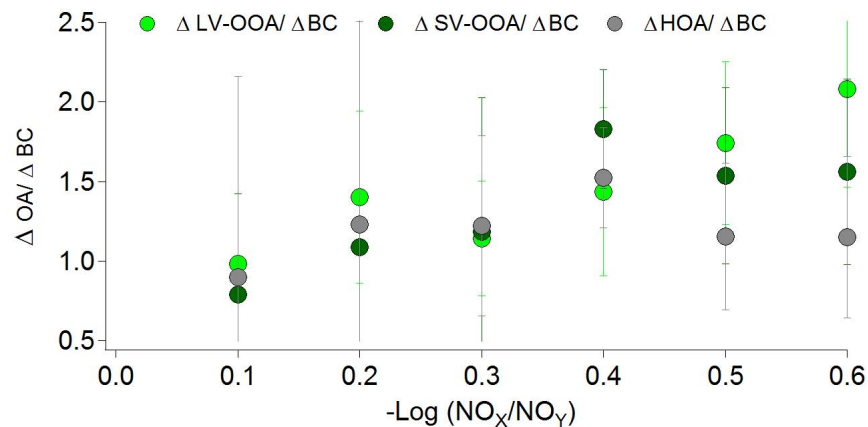


Fig. 6. The ratio ($\pm 1\sigma$) of $\Delta \text{LV-OOA}/\Delta \text{BC}$, $\Delta \text{SV-OOA}/\Delta \text{BC}$, and $\Delta \text{HOA}/\Delta \text{BC}$ as a function of photochemical age ($-\log(\text{NO}_x/\text{NO}_y)$).

Impact of urban emissions on regional aerosol particles

E. J. Freney et al.

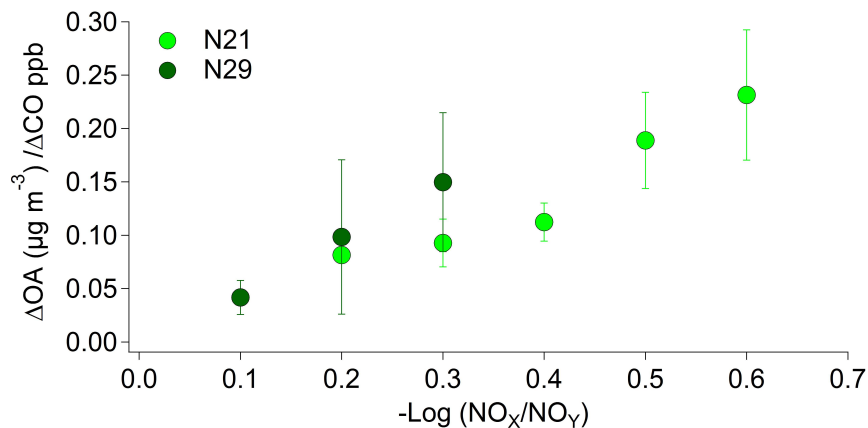


Fig. 7. The change in the $\Delta\text{OA} / \Delta\text{CO}$ for N21 and for N29 as a function of photochemical age.